A Stochastic Model for Soft Tissue Failure using Acoustic Emission data

D. Sánchez-Molina[a,*], E. Martínez-González[a], J. Velázquez-Ameijide[a], J. Llumà[a], M. C. Rebollo Soria[b], C. Arregui-Dalmases[a]

July 9, 2015

[a]UPC, Comte d'Urgell, 187, 08036 Barcelona, Spain
[b]IMLC, G.V. Corts Catalanes, 111, 08014 Barcelona, Spain

Abstract

The strength of soft tissues is due mainly to collagen fibers. In most collagenous tissues, the arrangement of the fibers is random, but has preferred directions. The random arrangement makes it difficult to make deterministic predictions about the starting process of fiber breaking under tension. When subjected to tensile stress the fibers are progressively straighten out and then start to be stretched. At the beginning of fiber breaking, some of the fibers reach their maximum tensile strength and break down while some others remain unstressed (this latter fibers will assume then major stress until they eventually arrive to their failure point). In this study, a sample of human esophagi was subjected to a tensile breaking of some fibers, up to the complete failure of the specimen. An experimental setup using Acoustic Emission to detect the elastic energy released is used during the test to detect the location of the emissions and the number of micro-failures per time unit. The data were statistically analyzed in order to be compared to a stochastic model which relates the level of stress in the tissue and the probability of breaking given the number of previously broken fibers (*i.e.* the deterioration in the tissue). The probability of a fiber breaking as the stretch increases in the tissue

*Corresponding author: david.sanchez-molina@upc.edu, Tel. +34 934137335

can be represented by a non-homogeneous Markov process which is the basis of the stochastic model proposed. This paper shows that a two-parameter model can account for the fiber breaking and the expected distribution for ultimate stress is a Fréchet distribution.

KEYWORDS: Collagenous Tissues, Acoustic Emission, Stochastic Failure Models, Esophagus.

1 Introduction

The non-linear elastic behavior of collagenous soft tissue is well understood, and complex models based on fiber arrangement have been developed [Natali *et al.*, 2009, Kroon & Holzapfel, 2008]. On the other hand, soft tissue failure shows a much more complex behavior. It is not so well understood and needs additional research [Ionescu *et al.*,2006]. The experimental data needed to develop models of failure are scarce and the adaptation of existing failure formulations for common engineering materials to soft tissues is difficult because of the micro-structure existing in soft collagenous tissues.

There are different types of soft tissue failure modes. The geometrical description of the last stages of failure has proved to be elusive with high degree of randomness. Reliable failure models is important for some medical procedures such as esophageal dilatation [Fernández-Esparrach *et al.*, 2011] and some other more unusual practical situations involving penetrating trauma injuries. This kind of injuries represents a high socioeconomic cost and represent a significant source of morbidity [Gugala & Lindsey,2003]

The present work focuses on the understanding of the cumulative effect of internal micro-failures before macroscopic failure. For this purpose a stochastic cumulative damage model based on inhomogeneous renewal-rewarded process is used (an inhomogeneous Markov process measures the number of micro-failures and the "reward" variables control the damage occurred in such a failure). The model presented here differs from other interesting probabilistic models found in the literature [Pradhan & Chakrabarti, 2003, Kabir *et al.*,2006] and is innovative in that it provides the distribution of the ultimate stress. On the other hand, another important innovation is the use of Acoustic Emission (AE) to detect experimentally almost all of the relevant micro-failures in soft tissues.

In section 2 the experimental setup is described and the two-parameter stochastic model is explained. Section 3 contains the results of the model applied to a human esophagus sample (the distribution for the ultimate stress is computed and the dissipated energy are given). Section 4 discusses the implications of the results.

2 Methods

A typical specimen of human esophagus from a donor (PMHS) was used for the experimental work. The age of the PMHS was 63 years-old, and its decease cause was not associated with any esophageal disease (biometric data: male; Body Mass Index, 25.5 kg·m^{-2}). This single sample produced $N = 472$ microfailures, which statistically is an adequate medium-size sample. A tensile test was conducted for the sample in order to obtain the stress-strain curve (the acoustic emission measurements and the strain-stress measures of the tensile test were simultaneous). A conventional servo-hydraulic testing machine (microtest EM2/20) was used for the measurement of force. The strain was computed from the data of a camera using motion tracking (see figure 1).

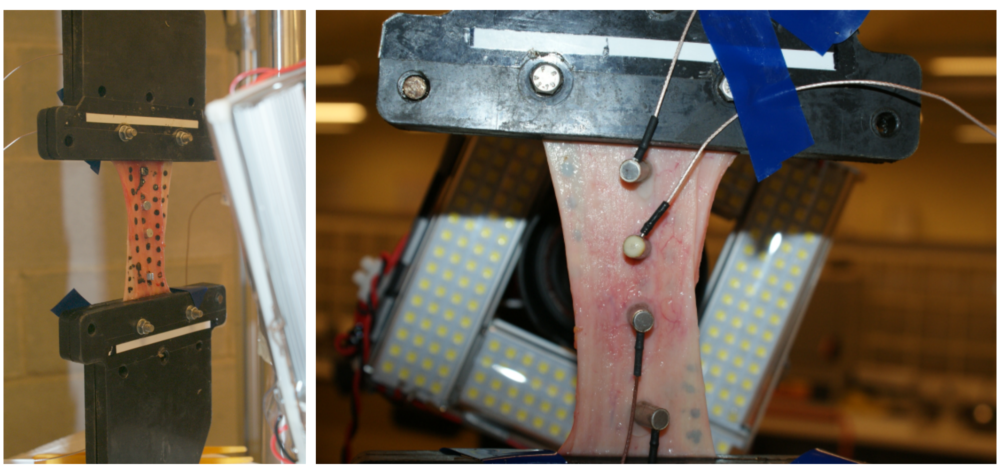

Figure 1: Experimental setting for the uniaxial tensile tests. *Right*: sample in place for testing, with clamps and acoustic sensors, the upright face is the *muscularis externa* layer. *Left*: detail of the acoustic sensors in the close-up face is the *mucosa* layer.

An important technical issue was the design of the clamps. The clamps were made out of non-porous polymeric material (Nylon 6) for two main reasons: (1) a porous material would have produced adherence and local dehydration in the sample, (2) in addition, being less rigid the polymeric material allows a better fit to the soft tissue. As it can be observed in figure 2, the planar clamps are formed by two sets of twin plates, each set is located at the edge of the rectangular sample of tissue. The clamps used for all tests were specifically designed for the occasion. The thickness and dimensions were adjusted in order to ensure that deformations of the clamps are completely negligible and the application of pressures and forces is fairly uniform. Preventing the creeping of the tissue was specially difficult because of the existence of water and moisture in the tissue; which in some cases acted as lubricant. After some preliminary testing and the addition of some extra drills the pressure was increased.

This pressure ensures no significant sliding and, thus, the strain measures are correct (if there had been any sliding, the strain measure would have been distorted). The experimental setting is the same described in [Sánchez-Molina *et al.*, 2014]. For the esophageal tissue, a stress-strain relation of type:

$$\tau = Ae^{-b\varepsilon^2}\varepsilon \tag{1}$$

was obtained the measured parameters were $A = 5385$ kPa and $b = 864.2$ (here τ is the [Piola] axial stress, and ε is the [Green-Lagrangian] strain). This relation 1 is deduced from the Yang-Gregersen-Deng constitutive equation [Deng *et al.*,1994, Yang *et al.*,2006], and it was found quite accurate ($r^2 = 0,9977$) for the data. For the purposes of this study, the exact constitutive equation used is not very important, as long as the model approximates well the stress-strain curve (all adequate models lead to a distribution function for the ultimate stress of the same type). The relation (1) is needed to calculate the stress when a failure is detected because the camera measures the strain, not the stress.

In addition, the experimental setup included four acoustic emission sensors (see Fig. 1) that detected the occurrence of micro-failures inside the sample (each micro-failure releases a certain amount of elastic energy which can be detected by sensors).

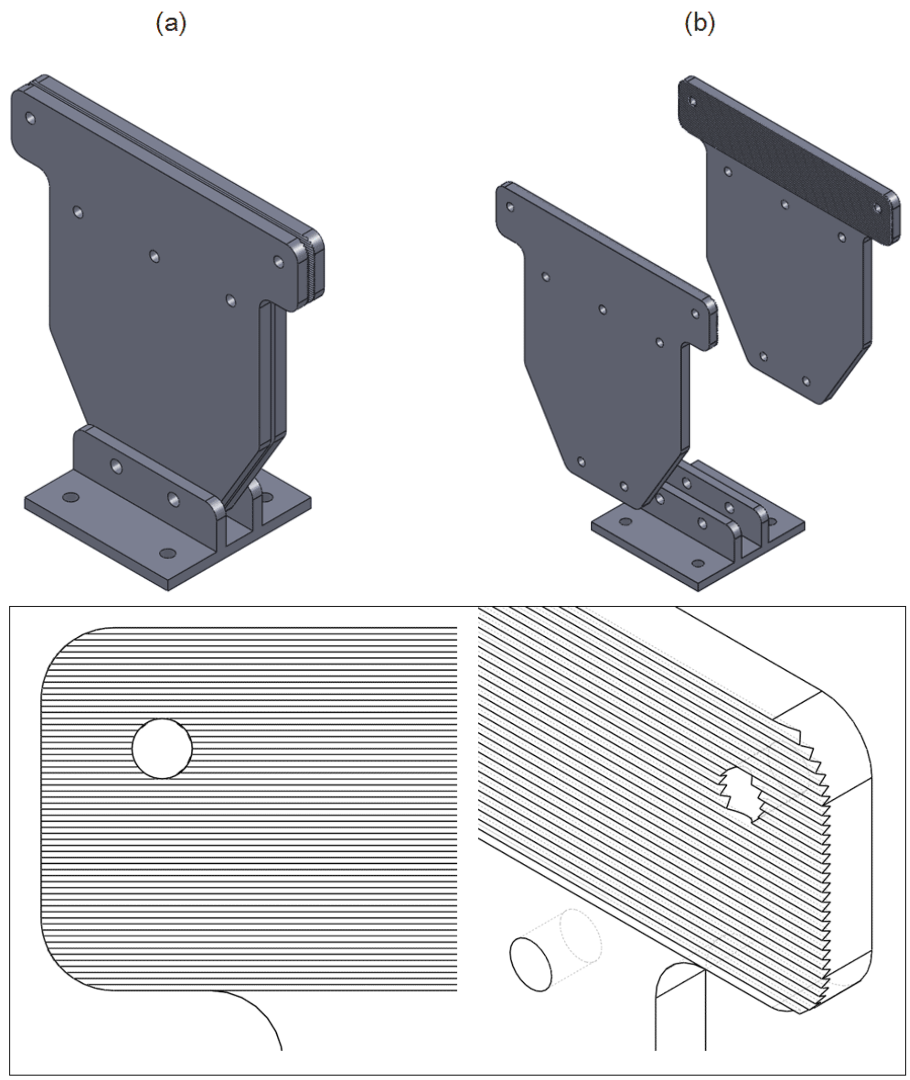

Figure 2: Planar clamps for uniaxial tensile tests: *Top* (a) the pair of clamps in position for holding the sample, (b) Exploded assembly. *Bottom* Details of the fluted surface.

2.1 Acoustic Emission Setup

The Acoustic Emission (AE) technique is a Non-Destructive Testing (NDT) method based on stress wave detection. Micro-structural damages or changes in an elastic material generate elastic waves that can be detected by AE

[Scruby, 1987, Drouillard,1996]. This technique has widely been used as an NDT in engineering applications and materials research, including use in biological tissue [Kohn, 1995, Paschos *et al.*, 1984]. AE is a very sensitive passive technique that does not interfere in the test. This makes it a specially useful technique and has been used for predicting failure of different types of materials, including composites and materials whose micro-structure contains fibers [Giordano *et al.*,1998, Huguet, *et al.*,2002].

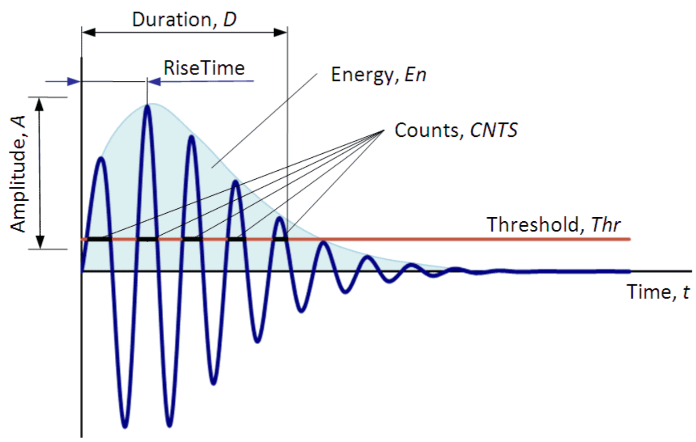

Figure 3: Main features of a stress wave detectable by acoustic emission. The threshold is used to discriminate relevant AE signals. The duration, the amplitude and the number of counts allow both the calculation of energy and the filtering of signals.

AE signals emitted during the tensile test were detected and recorded with a Vallen System Gmbh. Four miniature AE sensors were magnetically attached to the esophagus specimen (see Fig. 1). The sensors applied in the middle of specimen act as signal sensors while upper and lower sensors act as guard sensors to filter the signals from the grips. All four are of resonant type (VS700D, Vallen System Gmbh) with a frequency range between 100 – 800 kHz and a peak frequency of 600 – 800 kHz (flat range). Four 34 dB pre-amplifiers (AEP4) and four channel system (AMSY-5) were used. The AE system provides frequency filtering in the pre-amplifiers and on the AMSY-5 board. The filter is a band-pass type, and it was set to 95 – 850 kHz. The AE measurements were filtered using a low threshold of 34 dB, and signals with zero duration and/or zero rise time were removed (the AE signal features are shown in Fig. 3).

In this study, a detected signal whose energy exceeds the energy threshold and is almost "punctual in time" is called a *micro-failure*. It has been checked that visible breaking of fibers produces such a signal. We do not claim that every signal is the breaking of a single fiber. It could be that some of the micro-failures detected involve the breaking of groups of fibers. In fact, we have found that the micro-failures differ significantly in energy as it is reflected in equation (12).

2.2 Stochastic models

The fiber breaking process can be represented by means of two random variables (N_τ, D_τ) where N_τ represents the *number of micro-failures* (or number of "broken" fibers) and D_τ the *cumulative damage* when the level of stress is given by τ. The number of micro-failures N_τ is a [non-homogeneous] renewal process, *i.e.* a stochastic process constructed from a simple [non-homogeneous] Markov process [Whitt,1982]:

1. Let $S_1, S_2, \ldots, S_n$ be a sequence of increases in stress, S_{k+1} represents the stress increase between kth micro-failure and $(k+1)$−th micro-failure (we assume the expected values $\mathbb{E}(S_k)$ of the stress increases S_k are finite, $0 < \mathbb{E}(S_k) < \infty$).

2. Define for each n:

$$T_n = \sum_{i=1}^{n} S_i \tag{2}$$

   then T_n is the cumulative stress level at which the nth micro-failure occurs.

3. Finally the variable $N_\tau = \sup\{n | T_n \leq \tau\}$ the number of micro-failures up to the stress level τ.

Assume that the ith micro-failure involves a damage d_i (in practice, this is evaluated by the amount of energy released and detected by the AE sensors). Then the cumulative damage is given by

$$D_\tau = \sum_{k=1}^{N_\tau} d_k \tag{3}$$

The D_τ satisfies the conditions for being a [non-homogeneous] "renewal-reward process" (here the "reward" at kth step is the damage d_k), alternatively, some authors call this type of stochastic process a "shock process" [Aven & Jensen,1999, Klefsjö,1981]. In this study, the total damage D_τ is the total *dissipated energy* recorded by the AE sensors.

Some assumptions about the pair (N_τ, D_τ) are needed. First we assume that the random variables S_k are not identically distributed. The expected values of the variables satisfy:

$$\mathbb{E}[S_{k+1}] \leq \mathbb{E}[S_k] \tag{4}$$

This is so because after some micro-failures have occurred in a tissue there is some internal deterioration and the risk of an additional micro-failure increases. In addition, we assume that the stress increase between two successive micro-failure is due the so called "memoryless property":

$$\mathbb{P}(S_k > \tau_2 + \tau_1 | S_k > \tau_1) = \mathbb{P}(S_k > \tau_2) \tag{5}$$

where $\mathbb{P}(\cdot)$ denotes the probability measure. We can satisfy the condition (5) if for each k the random variable S_k follow an exponential distribution [Breuer & Baum,2005]. To deal with the condition (4), we introduced a feature used in the problem of machine maintenance developed in [Yeh,1988], where the time between two successive breakdowns decreases. The idea is to consider a deterioration parameter $a = \exp(\beta)$ [where $\beta > 0$ represents the "deterioration rate"] and to assume that "undeteriorated" random variables $\hat{S}_k$:

$$\hat{S}_k := S_k a^{k-1} = e^{\beta(k-1)} S_k \sim \mathrm{Exp}(\lambda) \tag{6}$$

are identically random variables distributed according to an exponential distribution: $\hat{S}_k \sim \mathrm{Exp}(\lambda)$ (i.e. all the variables $\hat{S}_k$ are distributed according to an exponential distribution of parameter $0 < \lambda < \infty$). Thus, in this study, the occurrence of micro-failures in time is modeled by a stochastic process with two parameters: λ and β. The exponential factor in (6) ensures a series of successive micro-failures with increasingly shorter "times" (stress increases) between micro-failures. These assumptions are qualitatively suggested by the observed behavior.

For the distribution function of the damage d_k associated with the kth micro-failure, the empirical distribution function is used. Therefore, the proposed model of failure is a stochastic process of type:

$$\{(N_\tau, D_\tau, \mathcal{F}_\tau) | \tau \in \mathbb{R}^+, (N_\tau, D_\tau) \in \mathbb{R}^2\} \tag{7}$$

where $\tau = \tau(\sigma_{ij})$ is the "equivalent stress" (i.e. a scalar function of the component of the stress tensor σ_{ij}), N_τ as defined above and D_τ given by (3). In the present case we used $\tau =$ the *first principal stress*. Formally, for each τ the triplet $(N_\tau, D_\tau; \mathcal{F}_\tau)$ is a random variable on $\mathbb{R}^2$ (here, $\mathcal{F}_\tau$ is the associated $\sigma-$algebra).

The experimental data are used to estimate the parameters of the model by comparing the current stress τ and the previous damage (the number of micro-failures N_τ and the cumulative damage D_τ). Obviously, as the stress and the cumulative damage increase, the stress span between any two consecutive micro-failures diminishes. The increasing probability per unit of time implies that we have a non-homogeneous continuous-time stochastic process. Note that in this model no hypothesis about the nature of fiber breaking is done.

2.3 Parameter Estimation

The proposed stochastic model has two defining parameters β and λ. The best fitting for these two parameters is computed by minimizing a penalty function $\phi(\beta, \lambda)$. The penalty function is a *sum of squares*. This penalty function has a minimum and the minimum is achieved for the best-fitting parameters. The procedure for finding the minimum of the penalty function is indeed a least-squares non-linear regression. The penalty function is given by the differences between expected values and sample values:

$$\phi(\beta, \lambda) = [\mu_\infty(\beta, \lambda) - \bar{\sigma}_u]^2 + \sum_{i=1}^{n} [\mu_{i,i+1}(\beta, \lambda) - (\sigma_{i+1} - \sigma_i)]^2 \tag{8}$$

where $\mu_{i,i+1}$ is the expected value of the stress increase between the i-th failure and the $(i+1)$-th failure, the σ_i are the corresponding actual experimental stresses. And $n = 470$ is given by the number of stress increasses between microfailures. Additionally, μ_∞ is the expected value of the stress increase between the first detected micro-failure and the ultimate stress; and $\bar{\sigma}_u$ is the corresponding observed increase.

The expected values μ_∞ and $\mu_{i,j}$ can be derived from (2)-(6). A computation of the expected values is presented in the Appendix [see equations (17) and (19)]:

$$\begin{cases} \mu_\infty = \dfrac{1}{(1-e^{-\beta})\lambda} \\ \mu_{i,j} = \dfrac{e^{-\beta(i-1)} - e^{-\beta j}}{(1-e^{-\beta})\lambda} \end{cases} \tag{9}$$

The best-fitting parameters were obtained by solving the system of non-linear equations:

$$\begin{cases} \dfrac{\partial\phi}{\partial\beta} = 0 \Rightarrow \quad [\mu_\infty - \bar{\sigma}_u]\dfrac{\partial\mu_\infty}{\partial\beta} + \sum_{i=1}^{n}[\mu_{i,i+1} - \sigma_{i+1} + \sigma_i]\dfrac{\partial\mu_{i,i+1}}{\partial\beta} = 0 \\ \dfrac{\partial\phi}{\partial\lambda} = 0 \Rightarrow \quad [\mu_\infty - \bar{\sigma}_u]\dfrac{\partial\mu_\infty}{\partial\lambda} + \sum_{k=1}^{n}[\mu_{i,i+1} - \sigma_{i+1} + \sigma_i]\dfrac{\partial\mu_{i,i+1}}{\partial\lambda} = 0 \end{cases} \tag{10}$$

3 Results

The solution of the nonlinear system 10 provides an estimation of the parameters λ and β. For solving it a Mapple 17 script was used. The procedure involves estimate initial values for $\lambda_0 \approx \lambda$ and $e^{-\beta_0} \approx e^{-\beta}$ and then a Newton-Raphson procedure was applied to compute λ and β. For both pre-estimation the equation (17) was used putting $\mu_\infty = t_\infty$, thus for the initial values λ_0 and β_0:

$$\lambda_0 := \frac{t_\infty}{1 - e^{-\beta_0}} \tag{11}$$

Then equation $\partial\phi(\lambda_0, \beta_0)/\partial\beta = 0$ is solved and a value β_0 is computed this also provides a value for λ_0 according to (11). These values were used to find solutions for $\beta \in [0, 100]$ and $\lambda \in (0, 10\lambda_0]$. This procedure had been tested for computed data with previously known values, and had proven to be robust for all the range of values.

The computed parameters for the sample of this study are $\beta = 0.0774$ and $\lambda = 0.0196$ [kPa^{-1}].

3.1 Number of micro-failures

The AE equipment provides a list of detected micro-failures or “hits” versus time. We can plot the number micro-failure versus measured stress (see Fig. 4).

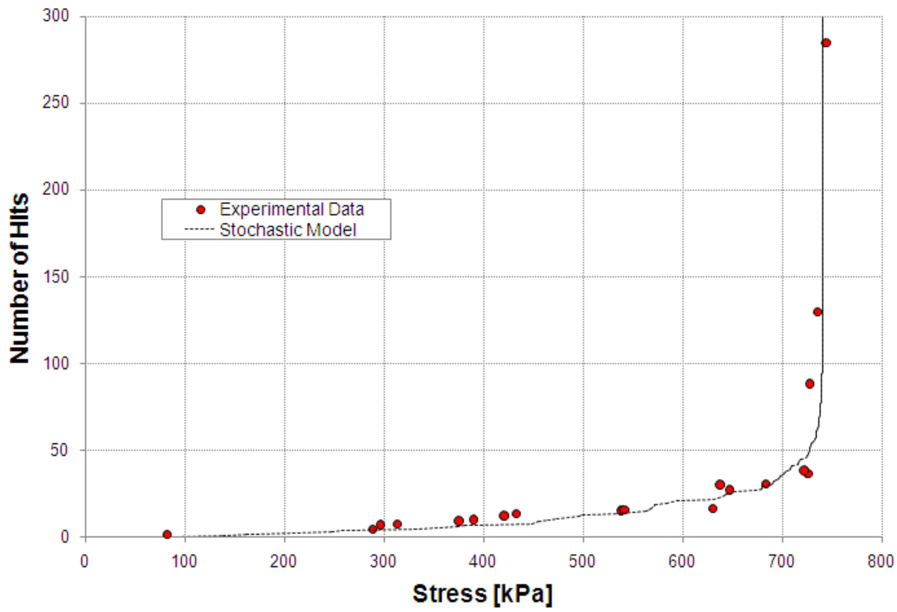

Figure 4: The number of micro-failures or hits versus the strain level, for a stress $\tau < 100$ kPa no micro-failures are observed (red spots). From this threshold, we observe some hits, and around $\tau \approx 720$ kPa an exponential increase in the number of micro-failures is observed. The dotted line correspond to a simulated curve using the computed parameters λ, β. The observed data and the simulated curve show high resemblance.

In figure 4, we see that a chain of successive micro-failures begins for $\tau > 100$ kPa, and then, the rate of micro-failures accelerates abruptly for $\tau \approx 720$ kPa, when the number of hits increases exponentially. Then, the cumulative effect of all these micro-failures around $\tau \approx 720$ kPa implies the rapid deterioration of the tissue and the final macroscopic failure. Thus in this model, the macroscopic failure is interpreted as a situation when a huge number of micro-failures are produced for a specific value of stress. The graphic for the number of micro-failures presents a vertical asymptote for the value at which macroscopic failure occurs. Namely, the ultimate stress if of the form $\sigma_u = \sigma_0 + T_\infty$ (where σ_0 is the threshold stress below which there is no fiber-breaking, and T_∞ is the limit random variable given by (2) when $n \to \infty$). This kind of catastrophic behavior is also found in other type of probabilistic models in the literature [Pradhan, & Hansen, 2005], although the probabilistic basis of these other models is different.

The next section shows that the "damage" or dissipated energy attains an arbitrarily high value when the number of micro-failures increases exponentially. Thus, after some prefixed level of damage, the tissue finally breaks down.

3.2 Distribution of dissipated energy

The same tendency can be seen for energy or damage (see Fig. 5). This figure shows the elastic energy lost in form of broken fibers. Around $\sigma \approx 720$ kPa. The tissue is unable to resist such an increase of damage and all the energy supplied by the test machine is occupied in breaking fibers. This finally causes the complete failure of the tissue.

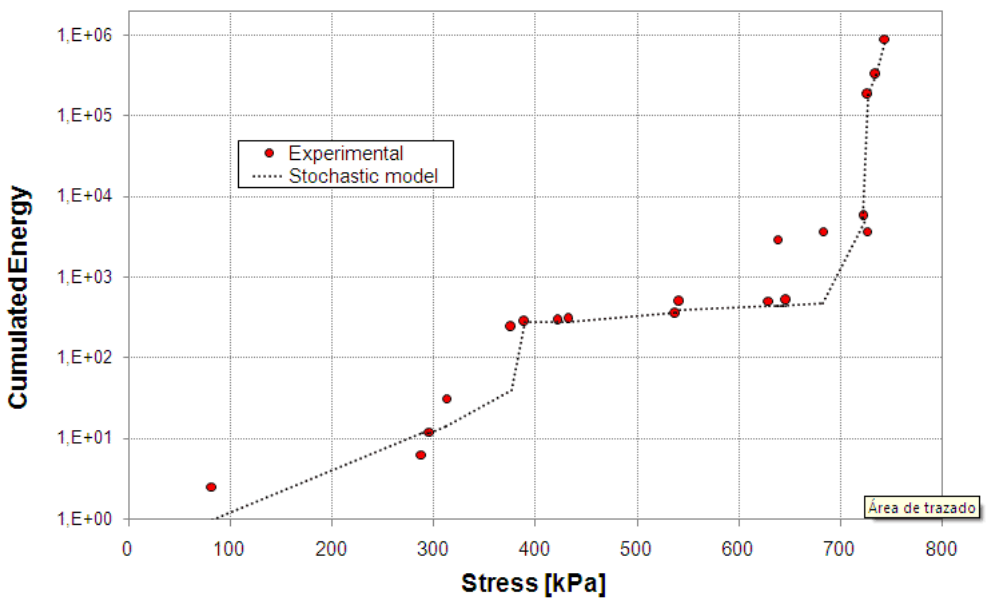

Figure 5: The dissipated energy in inelastic failures or breaking of fibers: red dots are the measured energies, and the dashed line is a simulated curve with the same parameters than the measured data.

In order to verify the accuracy of the model, the distribution of the *damage per micro-failure* E, i.e. the energy dissipated for each hit detected was investigated. As in other *critical phenomena* involving a high number of elements, the expected distribution of E was a power law or Pareto distribution (because, $\log(E)$ is exponentially distributed, see Fig. 6). The power law is a *scale-free* distribution. This kind of distributions is found in phase transi-

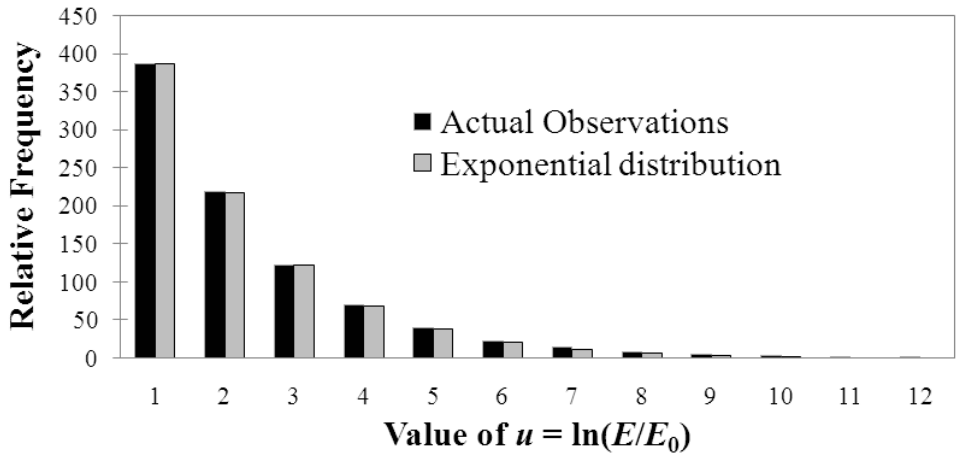

Figure 6: Histogram of the logarithm dissipated energy per micro-failure (u), compared to an exponential distribution with parameter $\alpha = 1.198$

tions [Uchino & Nomura,1982, Panagiotou *et al.*, 1984], economical crashes [Laloux *et al.*,2009], avalanches and other critically self-organized phenomena [Bak *et al.*,1988]. Other probabilistic models predicts the occurrence of avalanches of fiber failure [Pradhan, & Hansen, 2005] (but formal details of these models are different from the stochastic one presented in this paper). An accurate account of the data showed that the energies of micro-failures follow effectively a Pareto distribution of the form:

$$f_E(E) = \frac{\alpha}{E_0}\left(\frac{E_0}{E}\right)^{1+\alpha} \tag{12}$$

where α is a *decay parameter* and E_0 is an arbitrary constant depending on the units of energy used. Making the change $u = \ln(E/E_0)$, the equation (12) implies that the logarithm of the energy per micro-failure u is distributed according to an exponential law:

$$f_u(u) = \alpha \mathrm{e}^{-\alpha u} \tag{13}$$

This latter form is more convenient for finding the decay parameter α. The Fig. 6 shows a comparison the histogram for the actual observations of energy per micro-failure and the best-fitting exponential distribution for the observations. The fitting of the exponential distribution to the observations is very good (Kolmogorov-Smirnov test, and χ^2 test: $p > 0.9999$) and the computed parameter results to be $\alpha = 1.198$. This means that energy per micro-failure satisfies $\mathbb{P}(E > w) \propto w^{-1.198}$. As we pointed out in the section 2.1, this latter distribution refers to micro-failures and it is possible that some micro-failures involve groups of fibers.

3.3 Distribution of predicted maximum stress

It is interesting to note that even for given values of the model (β, λ), the maximum stress (σ_u) resisted by the tissue is not a fixed value, but it lies within a range because it is a stochastic model. So, it makes sense to look at the distribution of predicted maximum stress. A great number of simulations have been done $(n = 500)$ in order to generate the distribution of σ_u. We define previously, $\bar{\sigma}_u = \sigma_u - \sigma_0$ where σ_0 is the stress level for which the micro-failures begin. The simulations used a Montecarlo method for estimating a great number of values for variables of type $\hat{S}_k$ that are distributed according to an exponential distribution [see equation (6)], the variables $S_k = e^{-\beta(k-1)}\hat{S}_k$ were computed and the value of T_∞ is computed. By repeating this process $(n = 500)$, a good sample for $\bar{\sigma}_u$ is obtained.

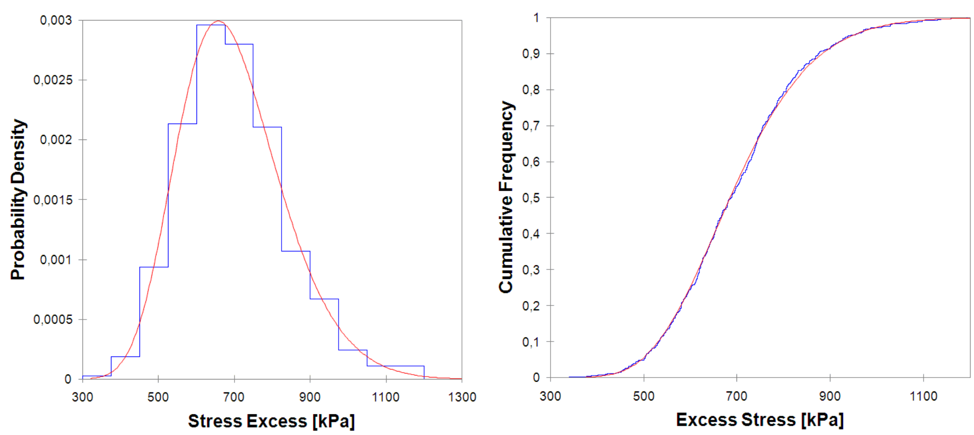

Figure 7: Empirical distribution for stress $\bar{\sigma}_u$ and adjusted model.

The empirical distribution (see Fig. 7) of $\bar{\sigma}_u$ seems to approximate pretty well to a Generalized Extreme Value distribution (GEV distribution) of Fréchet type, with cumulative distribution function:

$$F(\bar{\sigma}_u; \bar{\mu}, k, \xi) = \exp\left\{-\left[1 + \xi\left(\frac{\bar{\sigma}_u - \bar{\mu}}{k}\right)\right]^{-1/\xi}\right\} \tag{14}$$

The empirical parameters obtained from simulated data were $\xi = 0.146, k = 124.3$ kPa and $\bar{\mu} = 637.2$ kPa (Kolmogorov-Smirnov tests gives $p > 0.9944$). These values were estimated with a standard statistical package. Note that expected value is given by:

$$\begin{aligned} \mathbb{E}(\bar{\sigma}_u) &= \bar{\mu} + \frac{k}{\xi} - \frac{k}{\xi}\Gamma(1+\xi) \approx 693.1 \\ \mathrm{SD}(\bar{\sigma}_u) &= \frac{k}{\xi}\sqrt{\Gamma(1+2\xi) - \Gamma^2(1+\xi)} \approx 136.2 \end{aligned} \tag{15}$$

This is consistent with the expected value of the random variable $T_\infty[= \lim_n T_n]$. According to the Appendix we have:

$$\begin{aligned} \mathbb{E}(T_\infty) &= \frac{1}{(1-e^{-\beta})\lambda} = 693.62 \\ \mathrm{SD}(T_\infty) &= \frac{1}{\lambda}\frac{e^\beta}{\sqrt{e^{2\beta}-1}} = 135.18 \end{aligned} \tag{16}$$

The explicit derivation of the form of the equation (14) is discussed in the appendix, but the computations are not simple. For this reason we relied on numerical simulations.

4 Discussion

The model presented in this study can explain why the strength stress for a soft tissue material is not necessarily a fixed value, but a random variable with well defined distribution. The actual strength value obtained in one experiment will depend on very fine accidents in the intertwined fibers. In each experiment, the micro-structure is microscopically and highly random, for this reason not all the similar specimens present the same strength value. The best we can have is most likely a method for estimating the true distribution of strength, which is the main contribution of this article.

The idea of representing the mechanical failure by means of a probability density function is not new, however the way in which such a density is introduced in this article is innovative. Other authors have tried to explain the failure of materials (specially brittle and quasi-brittle ceramic materials) using probabilities, mainly, the Extreme Value theory (EV theory), and the Weibull distribution. Weibull distribution is a kind of Extreme

Value distribution. Many studies assume that at small scales the strength of the material is given by a distribution related to Weibull distribution [Sutcu,1989, Manzato *et al.*,2009]. Unlike these models, we do not assume special distributions at small scales instead we used a probabilistic machinery based on stochastic processes (and not directly on EV theory). The type of stochastic treatment used here allows to compute the parameters λ and β characterizing the original arrangement of fibers, and therefore, we can compute from them the distribution of ultimate stress by simulation. We found that the distribution of the strength of soft tissues is a Fréchet distribution, another type of Extreme Value distribution (indeed, Fréchet, Weibull and Gumbel distributions are the only three possible types of EV distributions and together they form the family of Generalized Extreme Value distributions).

However, it is possible that the GEV distributions are not the only type of distributions relevant for strength of materials. For example, an influent work in percolation models found a completely new type of distribution for the strength of the material [Duxbury *et al.*,1987]. Further work is needed to clarify how many the distributions are possible, our study shows that Fréchet distribution is one of the relevant distributions has to be considered.

Another interesting finding of this study is that fiber breaking in soft tissues present distributions of the same type found in other critical phenomena associated with a great number of elements in interaction, namely the presence of power-law or Pareto distributions. Further work is needed in order to interpret the decay parameter α, but it is interesting to note the presence of such an exponent in the distribution function of "damage".

About figures 4 and 5, it is important to highlight that we are dealing with stochastical, not deterministic processes. Thus, a simulation consists in a random sequence of microfailures, so the red dots represent the sequence of real microfailures in the tissue, and the dashed line is a simulated stochastical (random) curve using the same parameters computed for the sequence of real microfailures. In figure 4, both the simulated process and the observed process fit very well. In figure 5, both processes are qualitatively similar (but remember that red dots and the dashed line depict different instances of random processes with the same statistical parameters, so the dashed line is not an adjusted curve but only a qualitatively similar curve).

Finally, note that in this study, all the statistics are referred to the set of data of one specimen. The number of micro-failures ($n_{mf} = 285$) supplied by this specimen seems to be sufficient in order to achieve significance in various statistical tests. In addition, the adjusted parameters are adequate to generate a great number of different simulations ($n_{sim} = 500$). But it would be interesting to have different instrumented specimens in order to make inter-specimen statistics comparing the obtained parameters. Unfortunately, the current data does not allow such a comparison. A further step would be to obtain such data.

5 Appendix: Mean and Variance of T_∞

In this appendix we calculate the expected values and variances of the variables needed for the comparison with the experimental data and the fitting of the parameters in equation (8).

First, we consider the variable $T_\infty = \lim_n T_n$, where the variables T_n were defined in equation (2). The mean and the variance of this variable can be computed directly. For the mean $\mu = \mathbb{E}(T_\infty)$:

$$\mu_\infty = \mathbb{E}(T_\infty) = \mathbb{E}\left(\sum_{k=1}^{\infty} e^{-\beta(k-1)} \tilde{S}_k\right) = \sum_{k=1}^{\infty} e^{-\beta(k-1)} \mathbb{E}(\tilde{S}_k) = \frac{1}{(1-e^{-\beta})\lambda} \tag{17}$$

Second, for the computation of $\sigma_\infty^2 = \mathrm{Var}(T_\infty)$, we use $\sigma_\infty^2 = \mathbb{E}(T_\infty^2) - \mathbb{E}^2(T_\infty)$. We compute previously T_∞^2:

$$\begin{aligned} T_\infty^2 &= \left(\sum_{k=1}^\infty e^{-\beta(k-1)} \tilde{S}_k\right)^2 = \\ &= \sum_{k=1}^\infty \sum_{l=1}^k \left(\tilde{S}_l e^{-\beta(l-1)}\right)\left(\tilde{S}_{k+1-l} e^{-\beta((l+1-l)-1)}\right) \\ &= \sum_{k=1}^\infty e^{-\beta(k-1)} \sum_{l=1}^k \tilde{S}_l \tilde{S}_{k-l+1} \end{aligned}$$

Taking now expected values:

$$\begin{aligned} \mathbb{E}(T_\infty^2) &= \sum_{k=1}^\infty e^{-\beta(k-1)} \sum_{l=1}^k \mathbb{E}(\tilde{S}_l \tilde{S}_{k-l+1}) = \\ &= \sum_{k=1}^\infty \frac{e^{-\beta(k-1)}}{\lambda^2}\left(k + \frac{1+(-1)^{k+1}}{2}\right) \\ &= \frac{1}{\lambda^2(1-e^{-\beta})^2} + \frac{1}{\lambda^2(1-e^{-2\beta})} \end{aligned}$$

And, finally, we obtain using (17):

$$\sigma_\infty^2 = \mathbb{E}(T_\infty^2) - \mathbb{E}^2(T_\infty) = \frac{1}{\lambda^2}\frac{e^{2\beta}}{e^{2\beta}-1} \tag{18}$$

More in general, the random variables $T_{i,j}$ used for the fitting of parameters have expected values given by:

$$\begin{aligned} \mu_{i,j} = \mathbb{E}(T_{i,j}) &= \mathbb{E}\left(\sum_{k=i}^{j} e^{-\beta(k-1)}\tilde{S}_k\right) \\ &= \sum_{k=i}^{j} e^{-\beta(k-1)}\mathbb{E}(\tilde{S}_k) = \frac{e^{-\beta(i-1)} - e^{-\beta j}}{(1-e^{-\beta})\lambda} \end{aligned} \tag{19}$$

The above calculations are sufficient for adjusting parameters and showing the accuracy of the model. Another interesting question is to obtain directly the probability density distribution of T_∞. Technically, the probability distribution for the ultimate stress is computable but it involves infinite convolution products. In particular, some results of [Kawata, T. & Udagawa, M.,1949] can be used to obtain the *characteristic function* of the distribution of T_∞ which is the infinite product:

$$\varphi_{T_\infty}(s) = \mathbb{E}[e^{isT_\infty}] = \prod_{i=1}^{\infty}\left(1 - \frac{is}{\lambda e^{-\beta(k-1)}}\right)^{-1} \tag{20}$$

The computation necessary to write explicitly the probability function of T_∞ from the above expression is complex. For this reason, we have preferred numerical simulations to obtain the empirical distribution.

References

[Aven & Jensen,1999] Aven, T. & Jensen, U.: *Stochastic models in reliability* (book), ed. Springer, 1999.

[Bak *et al.*,1988] Bak, P., Tang, Ch., Wiesenfeld, K.: "Self-organized criticality", *Physical review A*, **38**(1), p. 364, 1988.

[Breuer & Baum,2005] Breuer, L. & Baum, D.: *An introduction to queueing theory and matrix-analytic methods* (book), ed. Springer, 2005.

[Deng *et al.*,1994] Deng, S.X., Tomioka, J., Debes, J.C., Fung, Y.C.: "New experiments on shear modulus of elasticity of arteries", *American Jour-*

nal of Physiology-Heart and Circulatory Physiology, **35**(1), pp. 1–10, 1994.

[Drouillard,1996] Drouillard, T.F. : “A history of acoustic emission”, *Journal of Acoustic Emission*, **14**(1), pp. 1–34, 1996.

[Duxbury *et al.*,1987] Duxbury, P.M., Leath, P.L., Beale, P.D.: “Breakdown properties of quenched random systems: The random-fuse network”, *Physical Review B*, **36**(1), p. 367, 1987.

[Giordano *et al.*,1998] Giordano, M., Calabro, A., Esposito, C., D’amore, A., Nicolais, L.: “An acoustic-emission characterization of the failure modes in polymer-composite materials”, *Composites Science and Technology*, **58**(12), pp. 1923–1928, 1998.

[Gugala & Lindsey,2003] Gugala, Z., and Lindsey, R. W.: “Classification of Gunshot Injuries in Civilians”, *Clin. Orthop. Relat. Res.*, **1**, pp. 65–81, 2003.

[Huguet, *et al.*,2002] Huguet, S., Godin, N., Gaertner, R., Salmon, L., Villard, D.: “Use of acoustic emission to identify damage modes in glass fibre reinforced polyester”, *Composites Science and Technology*, **62**(10), pp. 1433–1444, 2002.

[Ionescu *et al.*,2006] Ionescu, I., Guilkey, J. E., Berzins, M., Kirby, R. M. and Weis, J. A.: “Simulation of soft tissue failure using the material point method”, *Journal of biomechanical engineering*, **128**(6), pp. 917–924, 2006.

[Kabir *et al.*,2006] Kabir, M.R., Lutz, W., Zhu, K., Schmauder, S.: “Fatigue modeling of short fiber reinforced composites with ductile matrix under cyclic loading”, *Computational materials science*, **36**(4), pp. 361–366, 2006.

[Kawata, T. & Udagawa, M.,1949] Kawata, T. & Udagawa, M.: “On infinite convolutions”, *Kodai Mathematical Seminar Reports*, **1**, pp. 15–22, 1949.

[Klefsjö,1981] Klefsjö, Bengt.: “HNBUE survival under some shock models”, *Scandinavian Journal of Statistics*, pp. 39–47, 1981.

[Kohn, 1995] Kohn, D. H.: "Acoustic Emission and Nondestructive Evaluation of Biomaterials and Tissues", *Critical ReviewersTM in Biomedical Engineering*, **22**(3/4), pp. 221–306, 1995.

[Kroon & Holzapfel, 2008] Kroon and Holzapfel: "A new constitutive model for multi-layered collagenous tissues", *Journal of biomechanics*, **41**(12), pp. 2766–2771, 2008.

[Laloux *et al.*,2009] Laloux, L., Potters, M., Cont, R., Aguilar, J.-P., Bouchaud, J.-P.: "Are financial crashes predictable?", *Europhysics Letters*, **45**(1), 1999.

[Manzato *et al.*,2009] Manzato, C., Shekhawat, A., Nukala, P., Alava, M.J., Sethna, J.P., Zapperi, S.: "Fracture strength of disordered media: Universality, interactions, and tail asymptotics", *Physical review letters*, **108**(6), pp. 065504, 2012.

[Natali *et al.*, 2009] Natali, A. N., Carniel, E. L., and Gregersen, H.: "Biomechanical behaviour of oesophageal tissues: material and structural configuration, experimental data and constitutive analysis", *Medical engineering & physics*, **31**(9), pp. 1056–1062, 2009.

[Panagiotou *et al.*, 1984] Panagiotou, A.D., Curtin, M.W., Toki, H., Scott, D.K., Siemens, P.J.: "Experimental evidence for a liquid-gas phase transition in nuclear systems", *Physical Review Letters*, **52**(7), p. 496, 1984.

[Paschos *et al.*, 1984] Paschos, N.K., Aggelis, D.G., Barkoula, N.-M., Paipetis, A., Gartzonikas, D., Matikas, T.E.,Georgoulis, A.D.: "An Acoustic Emission Study for Monitoring Anterior Cruciate Ligament Failure Under Tension", *Physical Review Letters*, **53**(5), pp. 767–774, 2013.

[Hao *et al.*, 1984] Hao, D.-P., Tang, G., Xia, H., Xun, Zh.-P., Han, K.: "Avalanche process of the fiber-bundle model with stick-slip dynamics and a variable Young modulus", *Physical Review E*, **87**(4), pp. 042126, 2013.

[Pradhan & Chakrabarti, 2003] Pradhan, S. and Chakrabarti, B. K.: "Failure properties of fiber bundle models", *International Journal of Modern Physics B*, **17**(29), pp. 5565–5581, 2003.

[Pradhan, & Hansen, 2005] Pradhan, S. & Hansen, A.: "Failure properties of loaded fiber bundles having a lower cutoff in fiber threshold distribution", *Physical Review E*, **72**(2), pp. 026111, 2005.

[Sánchez-Molina *et al.*, 2014] Sánchez-Molina, D., Velázquez-Ameijide, J., Arregui-Dalmases, C., Rodríguez, D., Quintana, V., Shafieian, M. Crandall, J.R.: "A Microcontinuum Model for Mechanical Properties of Esophageal Tissue: Experimental Methodology and Constitutive Analysis", *Annals of biomedical engineering*, **42**(1), pp. 62–72, 2014.

[Fernández-Esparrach *et al.*, 2011] Fernández-Esparrach, G.,Córdova, H., Bordas, J. M., Gómez-Molins, I., Ginès, À., Pellisé, M., Sendino, O., González-Suárez, B., Cárdenas, Á., Balderramo, D.: "Manejo endoscópico de las complicaciones de la cirugía bariátrica. Experiencia tras más de 400 intervenciones", *Gastroenterología y Hepatología*, **34**(3), pp. 131–136; 2011, doi: 10.1016/j.gastrohep.2010.12.003

[Scruby, 1987] Scruby, C.B.: "An introduction to acoustic emission", *Journal of Physics E: Scientific Instruments*, **20**(8), pp. 946–953; 1987, doi: 10.1088/0022-3735/20/8/001.

[Sutcu,1989] Sutcu, M.: "Weibull statistics applied to fiber failure in ceramic composites and work of fracture", *Acta Metallurgica*, **37**(2), pp. 651–661, 1989.

[Uchino & Nomura,1982] Uchino, K., Nomura, Sh.: "Critical exponents of the dielectric constants in diffused-phase-transition crystals", *Ferroelectrics*, **44**(1), pp. 55–61, 1982.

[Whitt,1982] Whitt, W.: "Approximating a point process by a renewal process, I: Two basic methods", *Operations Research*, **30**(1), 1982.

[Yeh,1988] Yeh, Lam: "A note on the optimal replacement problem", *Advances in Applied Probability*, pp. 479–482, 1988.

[Yang *et al.*,2006] Yang, J., Zhao, J., Liao, D., Gregersen, H.: "Biomechanical properties of the layered oesophagus and its remodelling in experimental type-1 diabetes", *Journal of biomechanics*, **39**(5), pp. 894–904, 2006.